Mathematical Geology, Vol. 37, No. 6, August 2005 (© 2005)
DOI: 10.1007/s11004-005-7308-5

Estimating Regional Hydraulic Conductivity Fields—A Comparative Study of Geostatistical Methods[1]

Delphine Patriarche,[2] Maria Clara Castro,[2] and Pierre Goovaerts[3]

Geostatistical estimations of the hydraulic conductivity field (K) in the Carrizo aquifer, Texas, are performed over three regional domains of increasing extent: 1) the domain corresponding to a three-dimensional groundwater flow model previously built (model domain); 2) the area corresponding to the 10 counties encompassing the model domain (County domain), and; 3) the full extension of the Carrizo aquifer within Texas (Texas domain). Two different approaches are used: 1) an indirect approach where transmissivity (T) is estimated first and K is retrieved through division of the T estimate by the screen length of the wells, and; 2) a direct approach where K data are kriged directly. Due to preferential well screen emplacement, and scarcity of sampling in the deeper portions of the formation (>1 km), the available data set is biased toward high values of hydraulic conductivities. Kriging combined with linear regression, simple kriging with varying local means, kriging with an external drift, and cokriging allow the incorporation of specific capacity as secondary information. Prediction performances (assessed through cross-validation) differ according to the chosen approach, the considered variable (log-transformed or back-transformed), and the scale of interest. For the indirect approach, kriging of log T with varying local means yields the best estimates for both log-transformed and back-transformed variables in the model domain. For larger regional scales (County and Texas domains), cokriging performs generally better than other kriging procedures when estimating both (log T) and T*. Among procedures using the direct approach, the best prediction performances are obtained using kriging of log K with an external drift. Overall, geostatistical estimation of the hydraulic conductivity field at regional scales is rendered difficult by both preferential well location and preferential emplacement of well screens in the most productive portions of the aquifer. Such bias creates unrealistic hydraulic conductivity values, in particular, in sparsely sampled areas.*

KEY WORDS: kriging, cross-validation, lognormal kriging, transmissivity, specific capacity.

[1]Received 17 August 2004; accepted 2 December 2004.

[2]Department of Geological Sciences, University of Michigan, 2534 C. C. Little Building, Ann Arbor, Michigan 48109-1063; e-mail: delfpat@umich.edu; mccastro@umich.edu.

[3]BioMedware, 516 North State Street, Ann Arbor, Michigan 48104; e-mail: goovaerts@biomedware.com

INTRODUCTION

Hydraulic conductivity (K) is one of the parameters controlling both the magnitude and the direction of groundwater velocity, and consequently, is one of the most important parameters affecting groundwater flow and solute transport. Because it varies over at least 12 orders of magnitude (de Marsily, 1986), proper description of the internal properties of a groundwater system requires an accurate knowledge of the hydraulic conductivity field.

Direct and indirect measurements of hydraulic conductivity are commonly performed (e.g., Bredehoeft and Papadopulos, 1980; Neuzil, 1994; Wierenga, Hills, and Hudson, 1991), providing information on the magnitude of this parameter at the local scale (tens of cm to hundreds of m) and at shallow depths. Numerous geostatistical approaches have been proposed for generating maps of hydraulic property distributions at the local/shallow scale as inputs to numerical models of groundwater flow and mass transport (Fabbri, 1997; Koltermann and Gorelick, 1996; Lavenue and de Marsily, 2001). By contrast, field information on hydraulic conductivities at regional scales of tens to hundreds of kilometers and at greater depths ($>$1km) is relatively scarce. Hydraulic conductivity maps at such scales and depths are typically generated through numerical models that attempt to reflect the geological structure of the area and are simultaneously calibrated on both, hydraulic heads and natural tracer concentrations (e.g., Castro and Goblet, 2003; Castro and others, 1998a,b; Patriarche, Castro, and Goblet, 2004).

While numerical groundwater flow models are subject to the nonuniqueness problem, interpolation of field information is dependent on the quantity and quality of the available data set and on the chosen interpolation method. Geostatistical methods "tailor" the estimation process (kriging) of a regionalized variable according to its spatial correlation structure and allow for sparsely sampled observations of the variable of interest (primary information) to be complemented by a more densely sampled secondary attribute. Commonly, studies in which a comparative analysis of methodologies was undertaken have focused on the spatial structure of the log-transformed transmissivity (Aboufirassi and Marino, 1984; Ahmed and de Marsily, 1987; Christensen, 1997; Delhomme, 1974, 1979; Hughson, Huntley, and Razack, 1996; Wladis and Gustafson, 1999).

Here, we investigate the suitability of a diversity of geostatistical methods (ordinary kriging, ordinary kriging combined with linear regression, simple kriging with varying local means, kriging with an external drift, and ordinary cokriging) at interpolating log-transmissivities as well as log-hydraulic conductivities at regional scales and up to depths of 2 km. Such a comparative analysis is carried out in the Carrizo aquifer, a major groundwater flow system extending along Texas, in which all available primary (e.g., transmissivity, hydraulic conductivity) and secondary (specific capacity) information is used. Performance of different methods is evaluated at three regional levels/scales. These comprise the full extension of

the Carrizo aquifer within Texas (Texas domain), the domain corresponding to a three-dimensional groundwater flow model (model domain) previously built for simulation of groundwater flow and ^{4}He transport (cf. Patriarche, Castro, and Goblet, 2004), as well as the area corresponding to the 10 counties encompassing the model domain (County domain). Prediction performances of geostatistical procedures are evaluated by cross-validation for both log-transformed variables and back-transformed ones.

STUDY AREA AND AVAILABLE FIELD DATA

Geological and Hydrogeological Setting

The Carrizo aquifer, a major groundwater flow system, is part of a thick regressive sequence of terrigenous clastics that formed within fluvial, deltaic, and marine depositional systems on the northwestern margin of the Gulf Coast Basin (Fig. 1(A)). The Carrizo outcrops subparallel to the present day coastline, and follows a southwest–northeast wide band across Texas (Fig. 1(A)), dipping to the southeast where it reaches depths >2 km. The Carrizo aquifer terminates at a 32 km wide major growth-fault system, the Wilcox Geothermal Corridor (Fig. 1(A) and (B)). Groundwater flows gravitationally to the southeast, and discharge occurs by cross-formational upward leakage along the entire formation. The Carrizo sandstones, dominant in the outcrop area (90%), decrease gradually in the downdip direction, to reach a content of ∼20% in the growth-fault system area (Payne, 1972). The thickness of the Carrizo aquifer is highly variable, ranging from 50 m to ∼350 m.

Available Field Information and Quality Data Set

Our entire data set (cf. Mace and Smyth, 2003) results from pumping tests carried out in 702 wells located in the Texas domain (Fig. 1(A)). From these, 486 wells are located in the County domain (Fig. 1(A) and (B)) while 181 are part of the model domain (Fig. 1(B)). This data set includes historical records, some of which present incomplete field descriptions. Screen lengths are available for ∼80% of the wells (Table 1), while pumping test durations are described for 32 out of 63 wells where transmissivity is available. Pumping test duration varies from less than 1 h up to 48 h. Results issued from short-duration pumping tests are not representative of the entire thickness of the formation, rather, they reflect the local properties of the media in the vicinity of the well screen. Consequently, the hydraulic conductivity K (m s^{-1}) is given by:

$$K = \frac{T}{\mathrm{sl}} \tag{1}$$

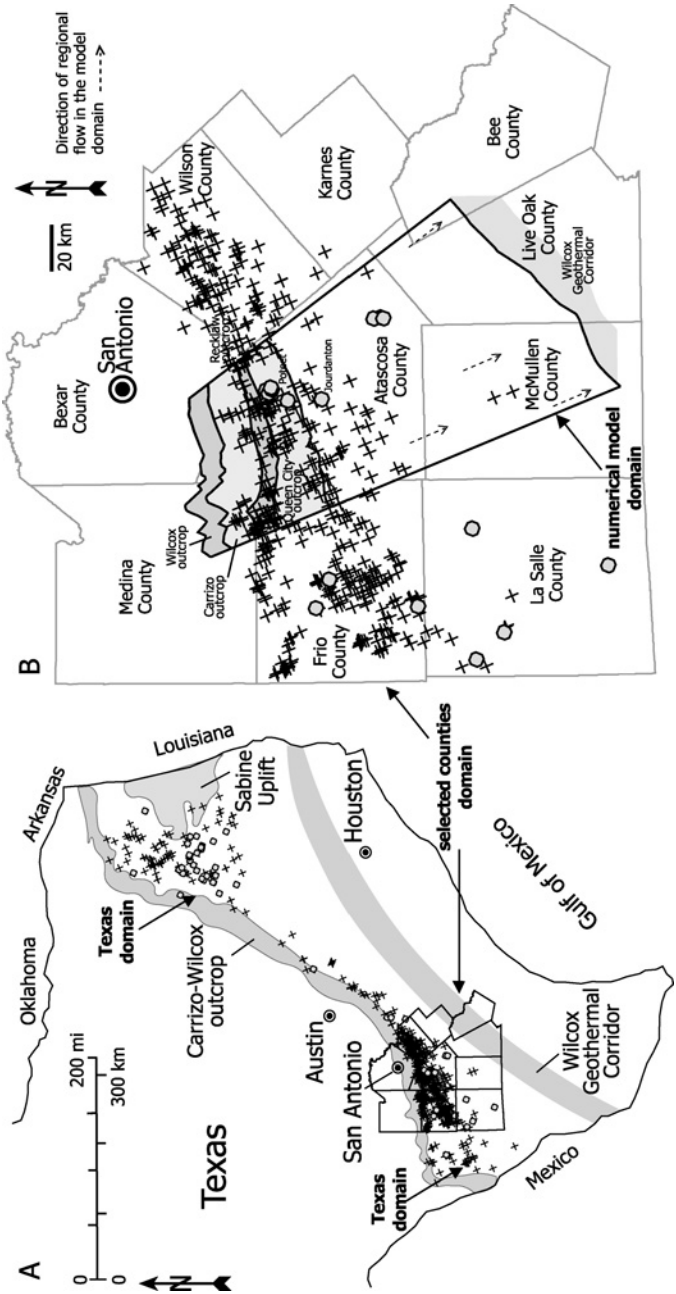

Figure 1. (A) Geographical setting of the Carrizo aquifer in Texas (after Hamlin, 1988). Locations of all wells tapping the Carrizo aquifer (Texas domain), where specific capacity (crosses) and transmissivity information (closed circles) are available (Mace and Smyth, 2003), are indicated. (B) Detailed view of the County domain with delineation of the model domain (cf. Patriarche, Castro, and Goblet, 2004), formation outcrops, and well locations.

Table 1. Number and Percentage of Wells with Information on Transmissivity, Specific Capacity, Screen Length, and Hydraulic Conductivity, for the Model, County, and Texas domains

Well information	Texas domain	County domain	Model domain
Transmissivity	63 (8.9%)	16 (3.3%)	9 (4.7%)
Specific capacity	692 (98.6%)	480 (98.7%)	187 (97.4%)
Screen length	559 (79.6%)	405 (83.3%)	159 (82.8%)
Hydraulic conductivity	24 (3.4%)	12 (2.5%)	9 (4.7%)
Total	702 (100%)	486 (100%)	192 (100%)

where T ($m^2\,s^{-1}$) is the transmissivity and sl (m) is the screen length of the well.

Information on both T and sl is available for only 24 wells in the Texas domain. From these, only 9 belong to the model domain. Scarcity of primary information (T and K) and incomplete records renders the use of secondary information necessary, as weighting the data to account for varying support scales (i.e., screen length) in the Carrizo aquifer is not a viable approach. In this particular case, secondary information is provided by the specific capacity SC ($m^2\,s^{-1}$), which is easy to obtain and for which a much more complete data set is available (cf. Table 1). Indeed, absence of meaningful T and K correlations with depth likely due to preferential sampling does not allow for the use of depth as secondary information. Similarly, because most K data available results from wells located within the 80–100% sand content region, use of sand-percentage as a secondary attribute is not possible. These, in turn, give origin to the presence of two main clusters (Fig. 1(A)), which are located in the highest sand content areas and at relatively shallow depths (<1 km). Despite this bias, hydraulic property estimations are directly made on the raw data set, as kriging procedures possess declustering properties (Journel and Huijbregts, 1978). In addition to preferential well locations, bias is also the result of preferential emplacement of well screens in the most productive portions of the aquifer (Mace and Smyth, 2003). Despite uncertainties on field measurements, we consider all transmissivity data obtained directly from pumping tests as "true" (i.e., exact and accurate), as opposed to those derived from specific capacity values, as described below.

Transmissivity Versus Specific Capacity

Analytical solutions (e.g., derived from the Dupuit–Thiem and/or Theis equations) predicting T from SC do not always agree well with "true" transmissivities as they neglect drawdown due to turbulent flow and generally lead to underestimated transmissivity values (Razack and Huntley, 1991). Empirical T–SC correlations give more accurate results (Huntley, Nommensen, and Steffey, 1992; Mace,

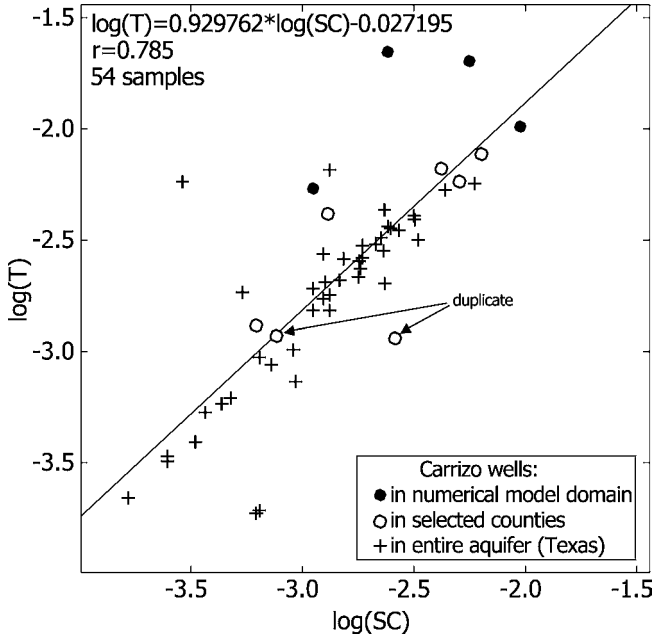

Figure 2. Log-specific capacity versus log-transmissivity, for the 53 wells where both data are available. Regression line, equation of the linear regression, and correlation coefficient are indicated.

1997). In addition, log–log functions yield greater correlation coefficients than linear functions (Razack and Huntley, 1991).

Empirical correlation $\log T$–$\log \mathrm{SC}$ for the Carrizo aquifer is based on 54 pumping tests performed on 53 wells where both parameters are available (Fig. 2). The linear regression equation is the following:

$$(\log\ T)_{\mathrm{reg}} = 0.929762 \times \log\ \mathrm{SC} - 0.027195 \tag{2}$$

The available duplicate (Fig. 2) presents a significant discrepancy between measured specific capacities (2.6×10^{-3} and $0.7 \times 10^{-3}\ \mathrm{m^2\ s^{-1}}$) while transmissivities are very similar (1.14×10^{-3} and $1.18 \times 10^{-3}\ \mathrm{m^2\ s^{-1}}$). This duplicate was considered in the determination of the linear regression (Eq. (2); correlation coefficient $= 0.785$) because transmissivities are consistent and variability in specific capacities inherent to field test conditions is represented.

For all wells where SC is available (692), $(\log T)_{\mathrm{reg}}$ (secondary information) was calculated using expression (2). The variance $\sigma^2_{(\log\ T)_{\mathrm{reg}}}$ of the regression

predictor is subsequently calculated through standard statistical analysis (e.g., Davis, 2002, p. 200–204).

Distribution of Primary and Secondary Attributes

Commonly, transmissivity and hydraulic conductivity data follow a log-normal distribution (Ahmed and de Marsily, 1987; Fabbri, 1997; Neuman, 1982). Despite data scarcity, transmissivity in the Carrizo aquifer presents a similar pattern (Fig. 3(A)). Although a normal distribution behavior is not required by kriging procedures, prediction performances are generally better when a strong skewness is not displayed by the sample distribution.

A base 10 logarithmic transform was applied to both transmissivity (Fig. 3(B)) and specific capacity data to mimic the approach traditionally followed by hydrogeologists. Although a normal score transform (Goovaerts, 1997) offers a more flexible way to handle asymmetric distributions, this type of transform and the associated multiGaussian kriging were not considered in this paper. In the Carrizo aquifer, the distribution of the log-transformed specific capacity is positively skewed, which is reflected on the $(\log T)_{\text{reg}}$ distribution (Fig. 3(C)). This observation strongly suggests that our specific capacity data are biased toward high values, likely due to preferential well locations as previously discussed.

METHODS

Semivariograms

Geostatistical techniques presented here capitalize on the presence of spatial correlation between data of the variable $Z = \log V$, where V is either the "true" transmissivity, or the hydraulic conductivity, or the specific capacity or yet, $\log V = (\log T)_{\text{reg}}$ computed according to expression (2).

Although all kriging systems introduced below are written in terms of covariances, common practice consists in inferring and modeling the semivariogram (that measures the dissimilarity between observations) rather than the covariance function. The experimental semivariogram $\hat{\gamma}(\mathbf{h})$ of Z for a given lag vector $\mathbf{h}$ is estimated as:

$$\hat{\gamma}_z(\mathbf{h}) = \frac{1}{2N(\mathbf{h})} \sum_{\alpha=1}^{N(\mathbf{h})} [z(\mathbf{u}_\alpha) - z(\mathbf{u}_\alpha + \mathbf{h})]^2 \tag{3}$$

where $N(\mathbf{h})$ is the number of data pairs within the class of distance and direction used for the lag vector $\mathbf{h}$. A continuous function must be fitted to $\hat{\gamma}(\mathbf{h})$ so as to deduce semivariogram values for any possible lag $\mathbf{h}$ required by prediction

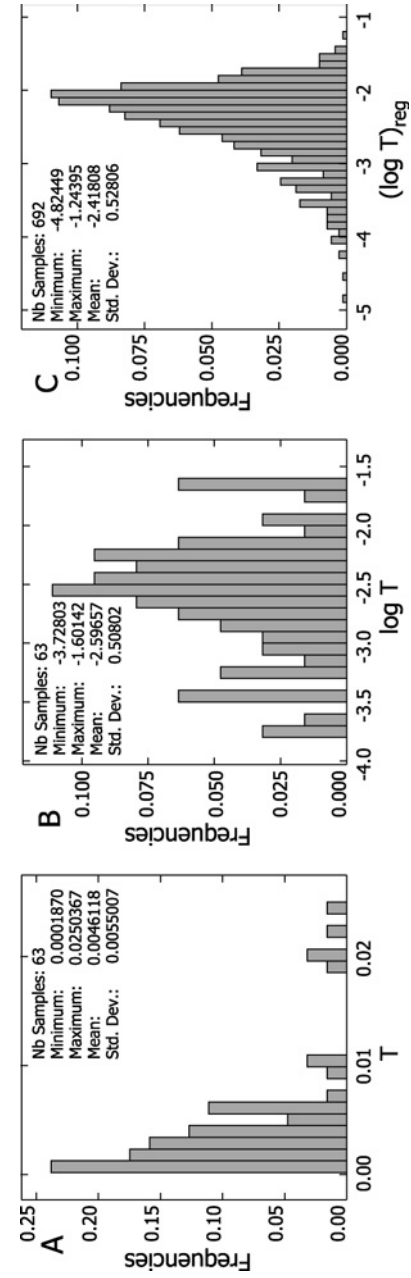

Figure 3. Frequency distributions of (*A*) transmissivity, (B) log-transmissivity, and (C) $(\log T)_{\text{reg}}$ obtained through linear regression on log-specific capacity information.

algorithms. All experimental semivariograms computed here refer to the entire data set, i.e., the Texas domain (Fig. 1(A)). Semivariogram models were fitted visually and estimations are performed using the software Isatis (Bleines and others, 2002). Although directional semivariograms computed for the densely sampled specific capacity indicates a slight anisotropy, all spatial fields will be modeled as isotropic because scarce primary information render the estimation of semivariogram of transmissivity and hydraulic conductivity very difficult.

Experimental semivariograms of $\log T$ and $\log K$ are fitted using an exponential model with a 10 km range (Fig. 4(A)), and a cubic model with a 12.5 km range (Fig. 4(B)), respectively. These range values are in agreement with previous findings (Anderson, 1997). Although T and K are considered as "true" data, a nugget effect reflecting the random variability of the parameters at a small scale is included in both semivariogram models.

All procedures used in this study to predict *in fine* the hydraulic conductivity field take into account, directly or indirectly, log-transformed specific capacities as secondary information. Structural analysis of $\log \mathrm{SC}$ and $(\log T)_{\mathrm{reg}}$ shows, not surprisingly, a very similar behavior since Equation (2) indicates that these two quantities are linearly related (Fig. 4(C) and (D)). Both theoretical semivariograms are exponential with 28 and 27 km ranges, respectively (Fig. 4(C) and (D)), and nugget effects (accounting for the measurement errors and the random variability at small scale) that represent about half of the model sills. Slight differences between both semivariograms are partly due to the number of wells considered for each one of them; the semivariogram of $\log \mathrm{SC}$ is calculated for all wells where specific capacity is available, while the semivariogram of $(\log T)_{\mathrm{reg}}$ is calculated for wells where only specific capacity is available (but not T).

Joint variability between primary and secondary variables Z and Y can be characterized using the experimental cross-semivariogram defined as:

$$\hat{\gamma}_{ZY}(\mathbf{h}) = \frac{1}{2N(\mathbf{h})} \sum_{\alpha=1}^{N(\mathbf{h})} [z(\mathbf{u}_\alpha) - z(\mathbf{u}_\alpha + \mathbf{h})][y(\mathbf{u}_\alpha) - y(\mathbf{u}_\alpha + \mathbf{h})] \tag{4}$$

The experimental cross-semivariogram of $\log T$ and $\log \mathrm{SC}$ is fitted using a linear model of coregionalization that includes an exponential model with an 8 km range and a nugget effect (Fig. 4(E)).

Interpolation Procedures

As mentioned earlier, estimation of hydraulic conductivity based only on primary information (log-transmissivity or log-hydraulic conductivity) is not adequate, as hydraulic conductivity is known only at a few locations and univariate prediction would yield very smooth maps that fail to reproduce the expected

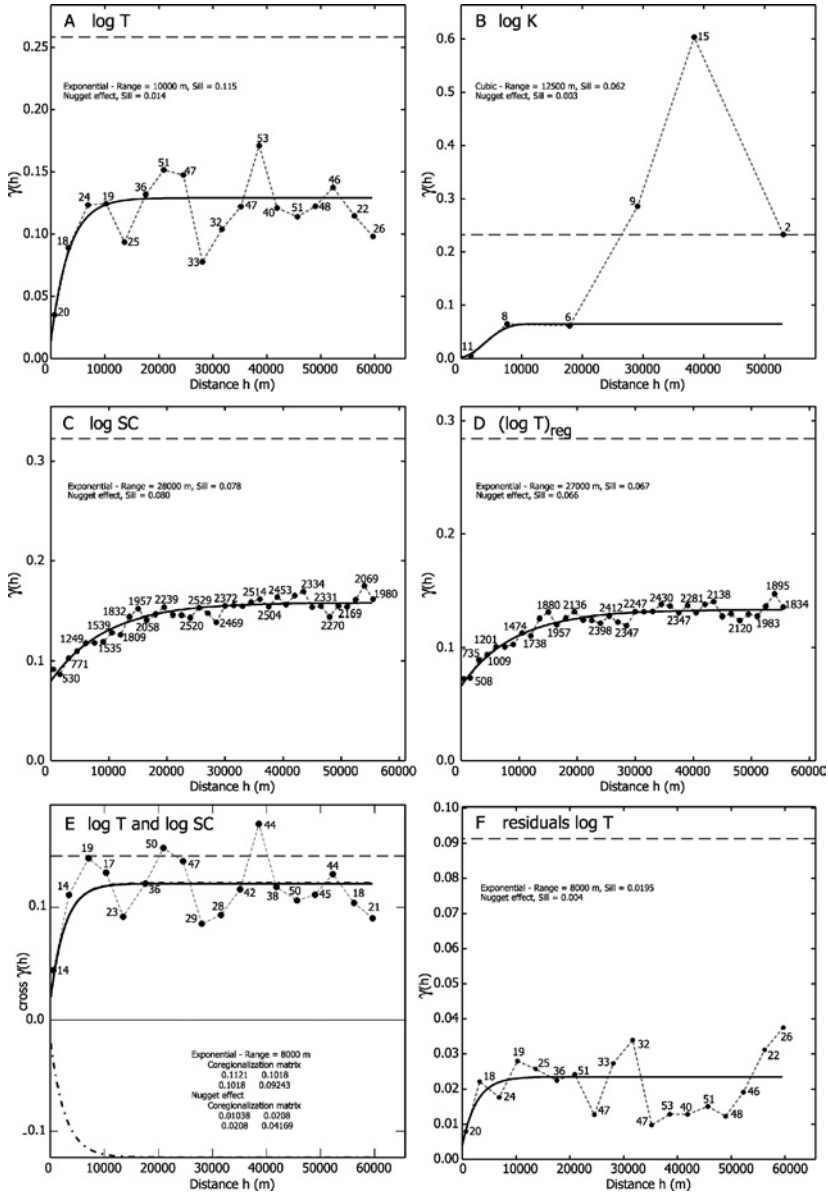

Figure 4. Experimental semivariograms and semivariogram models of (A) log-transmissivity, (B) log-hydraulic conductivity, (C) log-specific capacity, (D) $(\log T)_{\text{reg}}$, and (F) log-transmissivity residuals. (E) Experimental and modeled cross-semivariograms between log-transmissivity and log-specific capacity. Numbers of data pairs used per lag are indicated, as well as the structures, range, and sills of each semivariogram model.

variability obtained from both primary and secondary information. Several methods are available for incorporation of secondary information in the estimation procedure.

Kriging Combined with Linear Regression

First suggested by Delhomme (1974, 1979) and later discussed by Ahmed and de Marsily (1987), this procedure was used to combine measured or "true" transmissivity data with values obtained by linear regression of specific capacity, accounting for the regression errors. The kriging estimate $z^*(\mathbf{u})$ is as follows:

$$z^*(\mathbf{u}) = \sum_{\alpha=1}^{n(\mathbf{u})} \lambda_\alpha(\mathbf{u})\,(v(\mathbf{u}_\alpha) + e(\mathbf{u}_\alpha)) \tag{5}$$

where $n(\boldsymbol{u})$ is the number of neighboring z data used in the estimation, and $v(\mathbf{u}_\alpha)$ is the "true" transmissivity, $\log T$, at location $\mathbf{u}_\alpha$. Wherever the transmissivity has been measured and its true value is thus available, the error term $e(\mathbf{u}_\alpha)$ is zero. At other locations where the sole specific capacity is known, only uncertain transmissivity values are available, $v(\boldsymbol{u}_\alpha) + e(\boldsymbol{u}_\alpha) = (\log\ T)_{\text{reg}}$, and the error term corresponds to the unknown regression error. This method can thus be seen as a kriging with nonsystematic spatially uncorrelated errors (Chiles and Delfiner, 1999): zero at T data locations and non-zero at SC data locations. The weights $\lambda_\alpha(\mathbf{u})$, assigned to each observation, are computed by solving the following kriging system:

$$\begin{aligned}
&\sum_{\beta=1}^{n(\mathbf{u})} \lambda_\beta(\mathbf{u})\big[C(\mathbf{u}_\alpha - \mathbf{u}_\beta) + \delta_{\alpha\beta}\sigma^2_{(\log T)_{\text{reg}}}(\mathbf{u}_\alpha)\big] + \mu(\mathbf{u}) = C(\mathbf{u}_\alpha - \mathbf{u}) \\
&\alpha = 1, 2, \ldots, n(\mathbf{u}) \\
&\sum_{\beta=1}^{n(\mathbf{u})} \lambda_\beta(\mathbf{u}) = 1
\end{aligned} \tag{6}$$

where $\delta_{\alpha\beta} = 1$ if $\alpha = \beta$ and zero otherwise, $\sigma^2_{(\log\ T)_{\text{reg}}}(\mathbf{u}_\alpha)$ is the regression variance at location $\mathbf{u}_\alpha$, and the covariance function $C(\mathbf{h})$ is derived from the semivariogram model calculated only for "true" transmissivities inferred from fully described field tests (see details in Ahmed and de Marsily, 1987).

Simple Kriging with Varying Local Means (SKlm)

In this procedure, the secondary variable Y (or usually a function of it) is assumed to represent the local mean of the primary variable Z, i.e., $E[Z(\boldsymbol{u})] = Y(\boldsymbol{u})$.

The first step is to obtain at every interpolation grid node $\mathbf{u}$ the value of Y. In this paper, this was achieved by ordinary kriging (OK) of y-data (i.e., $(\log T)_{\text{reg}}$):

$$y^*_{\text{OK}}(\mathbf{u}) = \sum_{\alpha=1}^{n(\mathbf{u})} \lambda_\alpha^{\text{OK}}(\mathbf{u}) y(\mathbf{u}_\alpha) \tag{7}$$

where the weights are computed using a system of type (6) with $\delta_{\alpha\beta} = 0\ \forall\alpha,\beta$. The kriging estimate $y^*_{\text{OK}}(\mathbf{u})$ is then used as a local mean in the simple kriging (SK) of z-data:

$$\begin{aligned} z^*_{\text{SKlm}}(\mathbf{u}) &= \sum_{\alpha=1}^{n(\mathbf{u})} \lambda_\alpha^{\text{SK}}(\mathbf{u})[z(\mathbf{u}_\alpha) - y^*_{\text{OK}}(\mathbf{u}_\alpha)] + y^*_{\text{OK}}(\mathbf{u}) \\ &= \sum_{\alpha=1}^{n(\mathbf{u})} \lambda_\alpha^{\text{SK}}(\mathbf{u}) R(\mathbf{u}_\alpha) + y^*_{\text{OK}}(\mathbf{u}) \end{aligned} \tag{8}$$

where $R(\mathbf{u}_\alpha) = z(\mathbf{u}_\alpha) - y(\mathbf{u}_\alpha)$ are referred to as residuals. The kriging weights are obtained by solving the following simple kriging system:

$$\sum_{\beta=1}^{n(\mathbf{u})} \lambda_\beta^{\text{SK}}(\mathbf{u}) C_{\text{R}}(\mathbf{u}_\alpha - \mathbf{u}_\beta) = C_{\text{R}}(\mathbf{u}_\alpha - \mathbf{u}) \qquad \alpha = 1, 2, \ldots, n(\mathbf{u}) \tag{9}$$

where $C_{\text{R}}(\mathbf{h})$ is the covariance function of the residual random function $R(\mathbf{u})$, not that of the variable Z itself. In this procedure, the total variance of estimation equals the sum of the variances for the estimation of the y variable and the residuals, $\sigma^2_{y^*_{\text{OK}}}(\mathbf{u}) + \sigma^2_{R^*_{\text{SKlm}}}(\mathbf{u})$.

Kriging with an External Drift

Like the SKlm approach, kriging with an external drift (KED) uses the secondary information to derive the local mean of the primary attribute Z, then performs simple kriging on the corresponding residuals (Goovaerts, 1997). The main difference between both estimators is that in KED the linear relationship between primary and secondary variables is implicitly assessed through the kriging system within each search neighborhood. The KED estimate is computed as follows:

$$z^*_{\text{KED}}(\mathbf{u}) = \sum_{\alpha=1}^{n(\mathbf{u})} \lambda_\alpha(\mathbf{u}) z(\mathbf{u}_\alpha) \tag{10}$$

The weights $\lambda_\alpha(\boldsymbol{u})$, assigned to each observation, are computed by solving the following kriging system:

$$\begin{aligned}
&\sum_{\beta=1}^{n(\mathbf{u})} \lambda_\beta(\mathbf{u}) C_{\mathrm{R}}(\mathbf{u}_\alpha - \mathbf{u}_\beta) + \mu_0(\mathbf{u}) + \mu_1(\mathbf{u}) y(\mathbf{u}_\alpha) = C_{\mathrm{R}}(\mathbf{u}_\alpha - \mathbf{u}) \\
&\alpha = 1, 2, \ldots, n(\mathbf{u}) \\
&\sum_{\beta=1}^{n(\mathbf{u})} \lambda_\beta(\mathbf{u}) = 1 \\
&\sum_{\beta=1}^{n(\mathbf{u})} \lambda_\beta(\mathbf{u}) y(\mathbf{u}_\beta) = y(\mathbf{u})
\end{aligned} \tag{11}$$

where $\mu_1(\boldsymbol{u})$ and $\mu_2(\boldsymbol{u})$ are two Lagrange parameters accounting for the constraints on the weights. The residual covariance should be inferred from pairs of z-values that are unaffected or slightly affected by the trend. In this paper and in agreement with previous studies (i.e., Goovaerts, 2000), KED is performed using the same covariance model as SKlm.

Cokriging

Another technique for incorporation of secondary information is cokriging (CK), a multivariate extension of kriging. The main difference between cokriging and the previous geostatistical algorithms lies in how the secondary information is handled. Whereas in previous procedures the secondary attribute provides only information on the primary trend at location $\mathbf{u}$, it directly influences the cokriging estimate z^*, obtained as follows:

$$z^*_{\mathrm{CK}}(\mathbf{u}) = \sum_{\alpha=1}^{n(\mathbf{u})} \lambda_\alpha^{\mathrm{CK}}(\mathbf{u}) z(\mathbf{u}_\alpha) + \sum_{\alpha'=1}^{m(\mathbf{u})} \lambda_{\alpha'}^{\mathrm{CK}}(\mathbf{u}) y(\mathbf{u}_{\alpha'}) \tag{12}$$

The cokriging weights are the solutions of the following system of linear equations:

$$\begin{aligned}
&\sum_{\beta=1}^{n(\mathbf{u})} \lambda_\beta^{\mathrm{SK}}(\mathbf{u}) C_Z(\mathbf{u}_\alpha - \mathbf{u}_\beta) + \sum_{\beta'=1}^{m(\mathbf{u})} \lambda_{\beta'}^{\mathrm{SK}}(\mathbf{u}) C_{ZY}(\mathbf{u}_\alpha - \mathbf{u}_{\beta'}) + \mu_Z(\mathbf{u}) \\
&\quad = C_Z(\mathbf{u}_\alpha - \mathbf{u}) \qquad \alpha = 1, 2, \ldots, n(\mathbf{u})
\end{aligned}$$

$$\sum_{\beta=1}^{n(\mathbf{u})} \lambda_{\beta}^{\mathrm{SK}}(\mathbf{u}) C_{YZ}(\mathbf{u}_{\alpha'} - \mathbf{u}_{\beta}) + \sum_{\beta'=1}^{m(\mathbf{u})} \lambda_{\beta'}^{\mathrm{SK}}(\mathbf{u}) C_{Y}(\mathbf{u}_{\alpha'} - \mathbf{u}_{\beta'}) + \mu_{Y}(\mathbf{u})$$

$$= C_{YZ}(\mathbf{u}_{\alpha'} - \mathbf{u}) \qquad \alpha' = 1, 2, \ldots, m(\mathbf{u})$$

$$\sum_{\beta=1}^{n(\mathbf{u})} \lambda_{\beta}^{\mathrm{SK}}(\mathbf{u}) = 1$$

$$\sum_{\beta'=1}^{m(\mathbf{u})} \lambda_{\beta'}^{\mathrm{SK}}(\mathbf{u}) = 0 \tag{13}$$

An alternative not investigated in this paper is standardized ordinary cokriging where a single unbiasedness constraint is imposed, that is the sum of primary and secondary data weights equals one (Goovaerts, 1998).

Back-Transformation

Estimating the log-transform ($Z = \log V$) of a variable (V) is not an aim per se, and a back-transformation is needed to obtain the estimation of V. Unfortunately, if Z^* is the unbiased estimator of z, calculating the antilog back-transform of Z^* does not produce the unbiased estimation V^* of V. Instead of using the analytical expression for the lognormal back-transform (Journel, 1980), we adapted the empirical (and theoretically equivalent) approach proposed by Saito and Goovaerts (2000) for normal score back-transformation. Following the assumption underlying lognormal kriging, the estimator $Z^*(\mathbf{u})$ at location $\mathbf{u}$ follows a normal distribution defined by a mean and a variance equal to $z^*(\mathbf{u})$ and $\sigma^2_{z*(\mathbf{u})}$ (the estimation variance), respectively. This distribution is discretized using 100 quantiles $z_p(\mathbf{u})$ corresponding to probability $p = \frac{k}{100} - \frac{0.5}{100}$, with $k = 1, 2, \ldots, 100$. Then, the corresponding quantiles $v_{\mathrm{p}}(\boldsymbol{u})$ of the local distribution of V are calculated following:

$$v_{\mathrm{p}}(\mathbf{u}) = 10^{z_{\mathrm{p}}(\mathbf{u})} \tag{14}$$

Finally, the kriging estimate $v^*(\boldsymbol{u})$ is computed as follows:

$$v^*(\mathbf{u}) = \frac{1}{100} \sum_{k=1}^{100} v_{\mathrm{p}}(\mathbf{u}) \quad \text{with} \quad p = \frac{k}{100} - \frac{0.5}{100} \tag{15}$$

The variance $\sigma^2_{\mathrm{V}^*}(\mathbf{u})$ of the estimator $V^*(\mathbf{u})$ is calculated as follows:

$$\sigma^2_{\mathrm{V}^*}(\mathbf{u}) = \frac{1}{100} \sum_{k=1}^{100} (v_{\mathrm{p}}(\mathbf{u}))^2 - (v^*(\mathbf{u}))^2 \quad \text{with} \quad p = \frac{k}{100} - \frac{0.5}{100} \tag{16}$$

RESULTS AND DISCUSSION

Prediction performances for each algorithm are assessed using cross-validation (Isaaks and Srivastava, 1989), which consists in removing temporarily each sample from the data set, and in re-estimating it using the remaining data. Comparison criteria comprise the mean error (bias ME), the mean square error (MSE), and the mean relative error (MRE) of the estimate z^* and the back-transformed values v^*. For variable Z, these criteria are defined as follows:

$$\mathrm{ME} = \frac{1}{n}\sum_{\alpha=1}^{n}[z(\mathbf{u}_\alpha) - z^*(\mathbf{u}_\alpha)] \tag{17}$$

$$\mathrm{MSE} = \frac{1}{n}\sum_{\alpha=1}^{n}[z(\mathbf{u}_\alpha) - z^*(\mathbf{u}_\alpha)]^2 \tag{18}$$

$$\mathrm{MRE} = \frac{1}{n}\sum_{\alpha=1}^{n}\left|\frac{z(\mathbf{u}_\alpha) - z^*(\mathbf{u}_\alpha)}{z(\mathbf{u}_\alpha)}\right| \tag{19}$$

Although the various interpolators provide an error variance estimate, the latter is not retained as a performance criterion because in practice, it usually provides little information on the reliability of the kriging estimate (Armstrong, 1994; Journel, 1993).

Indirect Versus Direct Approaches

Hydraulic conductivity has been estimated using two different approaches: 1) an indirect approach where transmissivity is estimated first and K value is retrieved through division of the T estimate by the screen length, and 2) a direct approach where K data are kriged directly.

Indirect Approach

As mentioned earlier, the semivariogram model used in kriging combined with linear regression is the one calculated on data free of uncertainty (i.e., $\log T$; Fig. 4(A)). SKlm and KED algorithms are based on the semivariogram computed from the residuals $R(\mathbf{u}) = \log\ T(\mathbf{u}) - (\log\ T)_{\mathrm{reg}}(\mathbf{u})$. Due to incomplete records, only 53 residuals can be calculated (for wells where both $\log T$ and $(\log T)_{\mathrm{reg}}$ are available), even though $\log T$ is available at 63 locations. To account for the 10 remaining samples, we consider at these locations that $R(\mathbf{u}) = \log T(\mathbf{u}) - (\log T)^*_{\mathrm{reg}}(\mathbf{u})$, where $(\log\ T)^*_{\mathrm{reg}}$ is obtained beforehand by ordinary kriging. The experimental semivariogram of $\log T$ residuals $R(\mathbf{u})$ is fitted using an exponential model with an 8 km range and a nugget effect (Fig. 4(F)).

Cross-validation results for $(\log T)^*$ reported in Table 2 indicate that cokriging generally performs best, yielding to a more exact (lowest bias ME) and a more accurate (lowest MSE) $\log T$ estimation, independent of the considered domain. All methods using the semivariogram model of $\log T$ (kriging combined with linear regression, and ordinary kriging given for comparison) yield a mean error bias (ME) equal or higher than those of cokriging, with the lowest bias observed for KED. Such bias is dependent on the domain considered. Despite slightly larger mean errors, SKlm presents similar MSE and MRE when compared to cokriging. However, SKlm produces the lowest MRE on $\log T$ in the model domain.

Cross-validation results for the back-transformed variable T^* (Table 2) show that SKlm yields the smallest bias for the model domain, while the minimum bias for the County and Texas domains is obtained using cokriging of $\log T$ and $\log$ SC. Despite a higher mean bias on T^*, kriging combined with linear regression and SKlm generally produce more accurate results (lowest MSE) than cokriging. Interestingly, this contrasts and is the exact opposite of conclusions drawn from criteria calculated on $\log T$. Depending on the domain considered, MRE is minimized for different techniques, and none of the procedures can simultaneously produce the best results for all criteria in all three domains. Nevertheless, in the model domain, SKlm produces the most accurate results, with the minimum MSE (1.5×10^{-5}) and MRE (21.3%) values on T, despite a slightly higher mean bias (ME) as compared to the one obtained from $\log T$ and $\log$ SC cokriging. SKlm is therefore the method retained to estimate the log-transmissivity field $(\log T)^*$ in the model domain (Fig. 5(A)). The transmissivity field T^* is then calculated using the back-transformation of $(\log T)^*$ (Fig. 5(B)).

The hydraulic conductivity field over the model domain can be estimated by dividing the transmissivity field by the well screen length field. Due to the scarcity of wells at greater depths, direct kriging of the screen length may produce screen length estimates higher than the formation thickness itself. To overcome this difficulty, we perform the kriging of the ratios of the screen length over the formation thickness (th) where $r = \frac{\text{sl}}{\text{th}}$ is calculated for 159 wells in the model domain. Ratios range from 0.0246 to 0.974, with a mean value of 0.325. The experimental semivariogram of r is then fitted by an exponential model with a 38 km range and a nugget effect (Fig. 6(A)). The ratio r is estimated over the model domain using ordinary kriging and this semivariogram model. The screen length (Fig. 6(B)) is estimated as $\text{sl}^*(\mathbf{u}) = \text{th}(\mathbf{u}) \times r^*(\mathbf{u})$, where the formation thickness th is considered certain (error-free). Finally, the hydraulic conductivity field obtained through the indirect approach (Fig. 7) is computed as follows:

$$K^*(\mathbf{u}) = \frac{T^*(\mathbf{u})}{\text{sl}^*(\mathbf{u})} \tag{20}$$

Table 2. Mean Error, Mean Square Error, and Mean Relative Error of the Estimate $(\log T)^*$ Obtained by Cross-Validation, and of the Back-Transformed Estimate T^* for Each Interpolation Procedure, and for Each Domain (Model, County, and Texas Domains)

Procedure	Domain	Number of wells	ME log T	MSE log T	MRE log T(%)	ME T	MSE T	MRE T (%)
Ordinary Kriging (OK)	Model	9	0.233	0.103	12.9	3.9E-3	3.8E-5	23.2
	County	16	0.213	0.126	14.5	2.9E-3	2.6E-5	52.1
	Texas	63	0.023	0.108	10.4	4.9E-3	8.8E-6	97.3
Kriging combined with linear regression	Model	9	0.246	0.109	13.5	4.5E-3	4.4E-5	26.8
	County	16	0.188	0.104	13.1	2.8E-3	2.9E-5	45.1
	Texas	63	0.044	0.105	10.1	6.5E-4	9.6E-6	83.4
Simple Kriging with varying local means (SKlm)	Model	9	0.162	0.055	**8.6**	**4.3E-4**	**1.5E-5**	**21.3**
	County	16	0.108	0.061	9.5	−1.7E-4	**1.4E-5**	43.9
	Texas	63	0.066	0.096	9.5	−6.2E-5	**5.9E-6**	80.7
Kriging with external drift (KED)	Model	9	0.234	0.143	15.5	6.1E-4	8.5E-5	59.4
	County	16	0.111	0.069	8.9	−9.5E-4	4.0E-5	52.8
	Texas	63	**0.016**	0.054	**5.7**	−7.1E-5	1.1E-5	51.7
Cokriging log T–log SC (CK)	Model	9	**0.079**	**0.051**	9.0	4.7E-4	4.2E-5	40.7
	County	16	**0.062**	**0.052**	**8.6**	**3.8E-5**	3.0E-5	**40.2**
	Texas	63	0.021	**0.051**	6.7	**1.5E-5**	1.0E-5	**36.5**

Note. Bold indicates best results among all compared approaches.

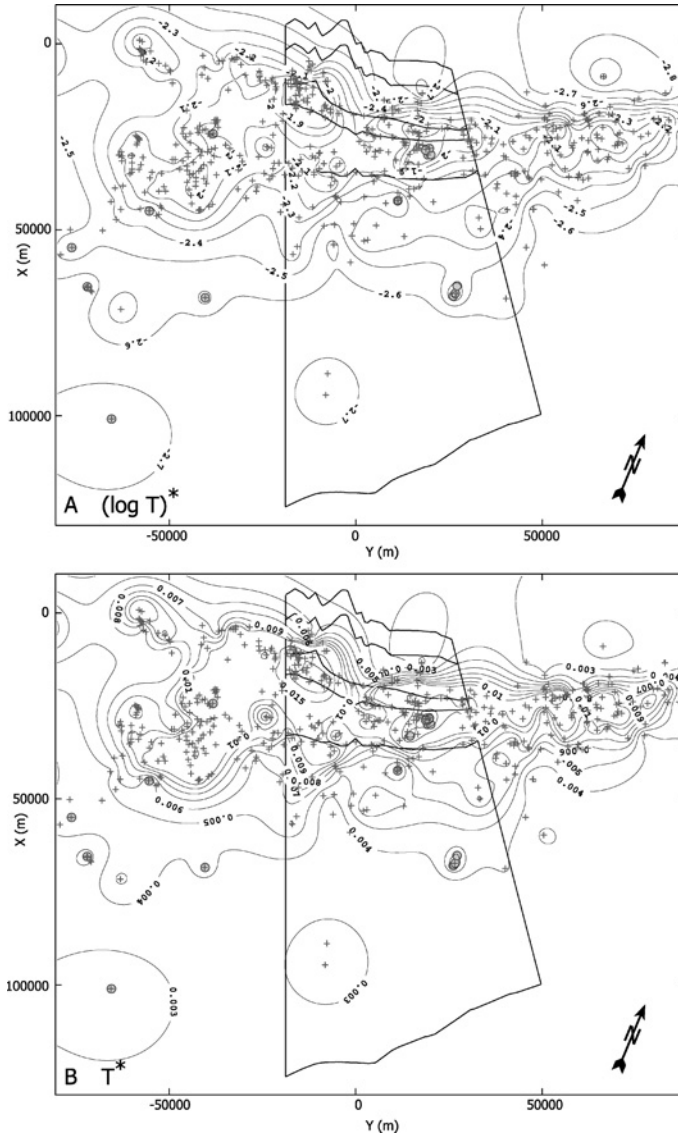

Figure 5. Map of $(\log T)^*$ estimated using SKlm of $\log T$ over the County domain. Symbols denote wells where specific capacity (crosses) and transmissivity (closed circles) are available. (B) Map of T^* ($m^2\,s^{-1}$) obtained from back-transformation of (A) over the County domain with delineation of the model domain, and well locations. Contour lines express constant variations of one unit inside each order of magnitude between 3×10^{-3} and $3 \times 10^{-2}\,m^2\,s^{-1}$; contour value of $1.5 \times 10^{-2}\,m^2\,s^{-1}$ is also indicated.

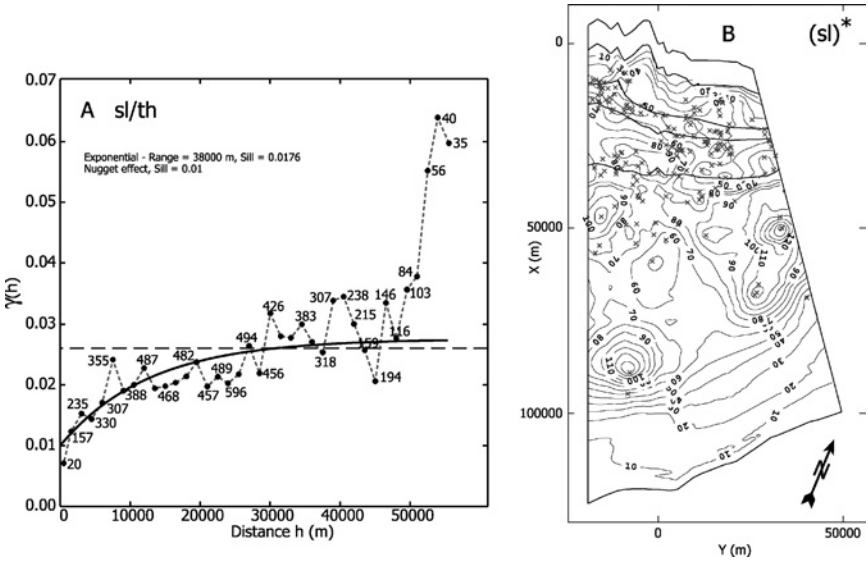

Figure 6. (A) Experimental and modeled semivariograms of the ratio of the screen length over the Carrizo thickness. Numbers of data pairs used per lag, and structure, range, and sill of the semivariogram model are indicated. (B) Map of the estimated screen length (sl)* in meters, corresponding to the productive thickness of the Carrizo in the model domain, obtained from the estimated ratio of the screen length (sl) derived from (A). Crosses denote wells in the model domain where screen length is available.

ME, MSE, and MRE for K^* using back-transformed T^* were calculated for all wells where screen length information was available in all three domains (Table 3). Results show that MRE values are less than 1% in the model and County domains, and below 2% in the Texas domain. Biases with respect to the mean of K values ($2.21 \times 10^{-4}\,\mathrm{m\,s^{-1}}$ on 24 data, in the Texas domain) remain small and vary between 7.2 and 16.2%.

Here, we have shown that the indirect approach produces good predictions of the hydraulic conductivity field. In the following section, we carry out a similar performance assessment for estimation of the hydraulic conductivity field through a direct approach.

Direct Approach

In the direct approach, the hydraulic conductivity field is estimated directly from hydraulic conductivity data. This approach is particularly challenging due to: a) small number of available primary data K (24), and b) the impossibility to use directly the specific capacity as secondary information. Thus, specific capacities

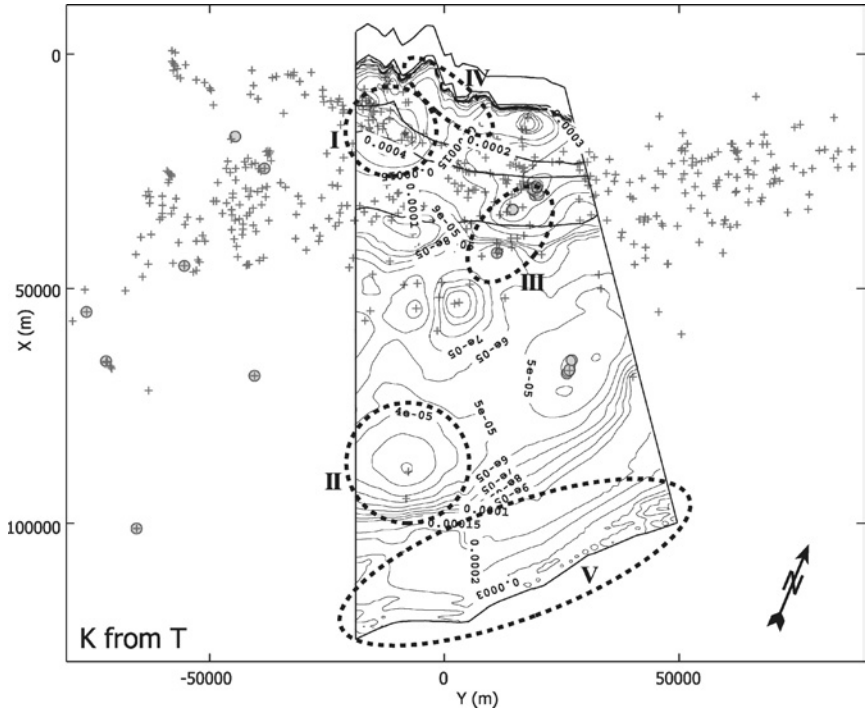

Figure 7. Map of the estimated K values (m s^{-1}) in the model domain obtained through the indirect approach, by dividing estimated $(\log T)^*$ values obtained from SKlm of $\log T$ (cf. Fig. 5(A)), by the estimation of the screen lengths (cf. Fig. 6(B)). Symbols denote wells where specific capacity (crosses) and transmissivity (closed circles) are available. Contour lines express constant variations of one unit inside each order of magnitude between 2×10^{-5} and 2×10^{-2} m^2 s^{-1}; contour value of 1.5×10^{-4} m^2 s^{-1} is also indicated.

are used indirectly and we define:

$$K_{\text{reg}} = \frac{T_{\text{reg}}}{\text{sl}} \quad \text{and} \quad \sigma^2_{K_{\text{reg}}} = \frac{1}{\text{sl}^2}\sigma^2_{T_{\text{reg}}} \tag{21}$$

K_{reg} is thus an approximate value of K that is obtained after back-transformation of $(\log T)^*_{\text{reg}}$. We calculate K_{reg} for all wells (550) where both screen length and specific capacity are available. $\sigma^2_{(\log T)_{\text{reg}}}$ is back-transformed to $\sigma^2_{T_{\text{reg}}}$ using Equations (14)–(16) for calculation of $\sigma^2_{K_{\text{reg}}}$. Finally, $\log(K_{\text{reg}})$ is calculated and $\sigma^2_{\log(K_{\text{reg}})} = \frac{1}{(\ln 10)^2} \ln(1 + \frac{\sigma^2_{K_{\text{reg}}}}{\overline{K_{\text{reg}}}^2})$. $\log K$–$\log(K_{\text{reg}})$ presents a correlation coefficient of 0.565 based on 15 samples where both variables are available.

Table 3. Mean Error, Mean Square Error, and Mean Relative Error of the Back-Transformed Estimates K^* Obtained Through the Indirect Approach

	Domain	Number of wells	ME K	MSB K	MRE K (%)
True screen length	Model	9	3.6E-5	1.9E-8	0.6
	County	12	1.6E-5	1.5E-8	0.6
	Texas	24	2.9E-5	1.3E-8	1.8

Note. K^* is calculated by dividing estimates of T obtained from cross-validation of simple kriging of $\log T$ residuals (cf. Table 2), by the true screen length of the wells, for each domain (Model, County, and Texas domains).

Identical procedures to those used for kriging $\log T$ are tested for $\log K$. Kriging combined with linear regression considers $\log K$ and $\log(K_{\text{reg}})$ as a unique variable, and it uses the previously fitted semivariogram model for $\log K$ (Fig. 4(B)). For SKlm and KED we consider the semivariogram computed from $R(\mathbf{u}) = \log\ K(\mathbf{u}) - \log(K_{\text{reg}})(\mathbf{u})$. Incomplete records prevent calculation of residuals at all 24 samples where $\log K$ is available. Consequently, for the 9 remaining samples a procedure similar to the one adopted in the indirect approach is applied. We use $R(\mathbf{u}) = \log\ K(\mathbf{u}) - \log(K_{\text{reg}})^*(\mathbf{u})$, where $\log(K_{\text{reg}})^*(\mathbf{u})$ is obtained beforehand by ordinary kriging (using the theoretical semivariogram presented in Fig. 8(A)). The semivariogram model of $\log K$ residuals is spherical with an 11 km range and no nugget effect (Fig. 8(B)). Here, scarcity of primary information makes it impossible to find a cross-semivariogram model that reasonably

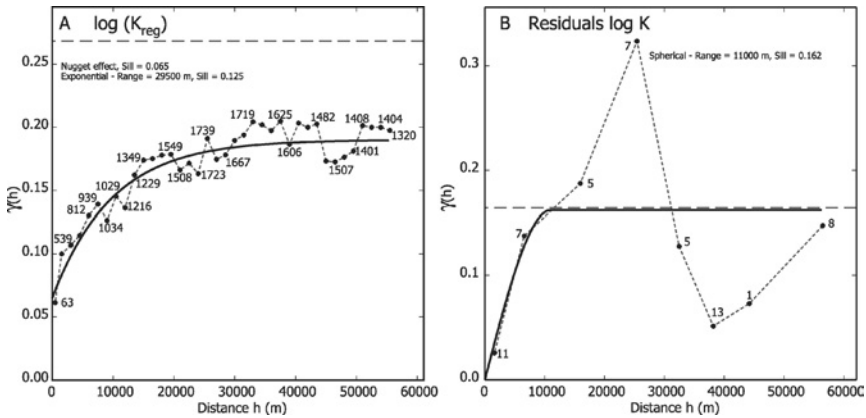

Figure 8. Experimental and modeled semivariograms of (A) $\log(K_{\text{reg}})$, and (B) $\log K$ residuals. Numbers of data pairs used per lag are indicated, as well as the structure, range, and sill of each semivariogram model.

Table 4. Mean Error, Mean Square Error, and Mean Relative Error of the Estimate $(\log K)^*$ Obtained by Cross-Validation, and of the Back-Transformed Estimate K^* for Each Interpolation Procedure, and for Each Domain (Model, County, and Texas Domains)

Procedure	Domain	Number of wells	ME $\log K$	MSE $\log K$	MRE $\log K$ (%)	ME K	MSE K	MRE K (%)
Ordinary kriging (OK)	Model	9	0.136	0.092	5.7	2.9E-4	1.3E-7	77.8
	County	12	0.048	0.112	5.8	2.2E-4	9.9E-8	87.6
	Texas	24	0.027	**0.130**	**6.8**	1.5E-4	5.8E-8	94.2
Kriging combined with linear regression	Model	9	0.331	0.253	11.3	2.0E-4	7.6E-8	59.8
	County	12	0.249	0.206	9.9	1.4E-4	5.8E-8	73.5
	Texas	24	0.247	0.220	10.1	9.6E-5	3.7E-8	**83.0**
Simple kriging with varying local means (SKlm)	Model	9	0.071	0.192	9.1	**−3.0E-5**	**4.6E-8**	119.2
	County	12	**−0.016**	0.185	9.0	**−9.0E-5**	6.4E-8	186.9
	Texas	24	**0.014**	0.205	9.8	−1.1E-4	7.2E-8	213.2
Kriging with external drift (KED)	Model	9	**0.069**	**0.038**	**5.1**	2.1E-4	6.9E-8	**50.2**
	County	12	−0.028	**0.037**	**4.5**	1.2E-4	**4.0E-8**	**43.2**
	Texas	24	0.032	0.158	7.8	**9.1E-5**	**3.1E-8**	85.5

Note. Bold indicates best results among all compared approaches.

fits the experimental $\log K$–$\log(K_{\text{reg}})$ cross-semivariogram. Thus, cokriging is not performed.

Comparison criteria include ME, MSE, and MRE computed from the cross-validation results of the log-transformed K and its back-transformed value. Results in Table 4 show that SKlm produces the minimum bias for the model and County domains. However, despite a fairly large bias, KED in the model and County domains appears to be the most reliable method with significantly better MSE and MRE on $\log K$, as well as a better MRE calculated on back-transformed K in these two domains. Thus, for the direct approach, maps of $\log K$ and K fields are produced using this interpolation technique (Fig. 9(A) and (B), respectively).

Comparison of Estimation Approaches in the Model Domain

Although indirect and direct approaches are rather distinct in their respective estimation procedures for $\log T$ and $\log K$, the resulting hydraulic conductivity fields display identical spatial variability (e.g., areas I and II; Figs. 7 and 9(B)) and thus, similar patterns. However, significant local discrepancies are present concerning the connectivity of high hydraulic conductivity areas (III; Figs. 7 and 9(B)). This is because when considering $r = \frac{\text{sl}}{\text{th}}$, the indirect approach introduces a structural control of hydraulic conductivity over the entire model domain. This is particularly significant in the outcrop area (IV, Fig. 7), as an artificial increase of the hydraulic conductivity is indirectly induced by a thickness decrease as one

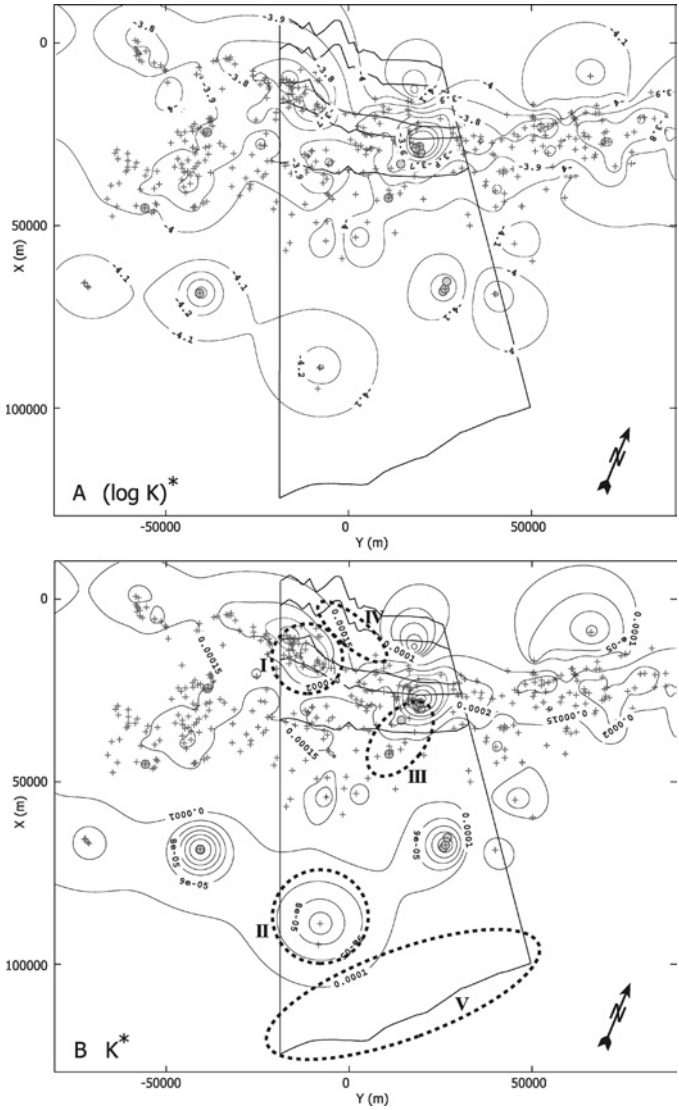

Figure 9. (A) Map of estimated $(\log K)^*$ values over the County domain obtained through the direct approach, using kriging of $\log K$ with an external drift. Wells where K_{reg} (crosses) and hydraulic conductivity K (closed circles) are available are indicated. (B) Map of K^* ($\mathrm{m\,s^{-1}}$) obtained over the County domain from back-transformation of (A). Delineation of the model domain and well locations are indicated. Contour lines express constant variations of one unit inside each order of magnitude between 3×10^{-5} and $6 \times 10^{-4}\,\mathrm{m\,s^{-1}}$; contour values of 1.5×10^{-4} and $2.5 \times 10^{-4}\,\mathrm{m\,s^{-1}}$ are also indicated.

gets closer to the outcrop limit (th $\rightarrow$ 0, $r \rightarrow \infty$). In this area and despite data sparsity, the direct approach produces a more realistic hydraulic conductivity pattern (Fig. 9(B)). Similarly, scarcity of data is an issue at the vicinity of the Wilcox Geothermal Corridor (V, Figs. 7 and 9(B)). Thus, in these areas, estimations of the aquifer properties are obtained through extrapolation and produce hydraulic conductivity estimates that increase as the Carrizo dips down, to reach depths >2 km and sand content of $\sim$20% (Payne, 1972), resulting in hydraulic conductivities at great depths (Fig. 7) as high as those estimated in the outcrop area. Such observation is in contradiction with expected hydraulic conductivity behavior due to compaction and diagenetic processes (e.g., Patriarche, Castro, and Goblet, 2004).

Independently of the chosen geostatistical method and approach, data scarcity and preferential sampling do not allow a good reproduction of hydraulic conductivity–depth dependence, making the estimation of hydraulic properties in the deepest portions of the aquifer unreliable. By contrast, the estimated hydraulic conductivity field in the shallower portions of the aquifer, where secondary information is largely available, is reliable. Specifically, in the model domain, SKlm (indirect approach) yields the best estimation.

CONCLUSION

Five geostatistical methods (ordinary kriging, ordinary kriging combined with linear regression, simple kriging with varying local means, kriging with an external drift, and cokriging) are tested for interpolation of the hydraulic conductivity field over domains of increasing extent within the Carrizo aquifer, in Texas. Two distinct approaches are used in this estimation: a) indirect approach in which transmissivity is used as primary information; and, b) direct approach, where hydraulic conductivity is treated as primary information. Although all procedures used log-transformed variables and incorporate secondary information derived from specific capacity data, methods with the best prediction performances (established through cross-validation) differ according to the chosen approach, the considered variable (log-transformed or back-transformed), and the domain (scale) of interest.

Kriging of $\log T$ residuals (SKlm) following the indirect approach yields the best estimates for both log-transformed and back-transformed variables in the model domain. For larger regional scales (County and Texas domains), cokriging performs generally better than univariate kriging procedures when estimating both $(\log T)^*$ and T^*. Scarcity of primary K data prevents estimation of $\log K$ by cokriging through the direct approach, and in this case the best prediction performances are obtained using kriging of $\log K$ with an external drift. Cross-validation also indicates that the indirect approach leads to smaller prediction errors than the direct approach, which is likely due to fewer available K primary

data as well as a weaker correlation between primary and secondary attributes in the direct case.

This paper has introduced several procedures that allow the combination of various types of information (hydraulic conductivity, transmissivity, specific capacity, screen length) in the spatial interpolation of hydraulic parameters. None of these techniques provides systematically better predictions for all scales, which stresses the importance of using cross-validation to compare performances of alternative approaches and assess the unbiasedness of the back-transform procedure.

Overall, estimation of the hydraulic conductivity field at such large regional scales through the tested geostatistical methods appears to be extremely difficult due to both preferential well location and preferential emplacement of well screens in the most productive portions of the aquifer. For example, in the deepest portions of the aquifer in the model domain, the estimated hydraulic conductivity field is obtained by extrapolation and gives origin to unrealistically high hydraulic conductivity values.

ACKNOWLEDGMENTS

The authors wish to thank R. E. Mace (Texas Water Development Board, Austin) for his help in providing geological and hydrogeological information. Financial support by the U.S. National Science Foundation Grant No. EAR-03087 07, the Elizabeth Caroline Crosby Research Award (NSF ADVANCE at the University of Michigan), and the "Ministère des Affaires Etrangères," France, for D. Patriarche through the program "Bourse Lavoisier," is greatly appreciated.

REFERENCES

Aboufirassi, M., and Marino, M. A., 1984, Cokriging of aquifer transmissivities from field measurements of transmissivity and specific capacity: Math. Geol., v. 16, no. 1, p. 19–35.

Ahmed, S., and de Marsily, G., 1987, Comparison of geostatistical methods for estimating transmissivity using data on transmissivity and specific capacity: Water Resour. Res., v. 23, no. 9, p. 1717–1737.

Anderson, M. P., 1997, Characterization of geological heterogeneity, *in* Dagan, G., and Neuman, S. P., eds., Subsurface flow and transport; a stochastic approach, International Hydrology Series: Cambridge University Press, Cambridge, U.K., v. 5, p. 23–43.

Armstrong, M., 1994, Is research in mining geostats as dead as a dodo? *in* Dimitrakopoulos, R., ed., Geostatistics for the next century, Quantitative Geology and Geostatistics: Kluwer Academic, Dordrecht, The Netherlands, v. 6, p. 303–312.

Bleines, C., Deraisme, J., Geffroy, F., Jeannée, N., Perseval, S., Rambert, F., Renard, D., and Touffait, Y., 2002, ISATIS Software Manual, 4th ed.: Géovariances, Fontainebleau, France, 645 p.

Bredehoeft, J. D., and Papadopulos, S. S., 1980, A method for determining the hydraulic properties of tight formations: Water Resour. Res., v. 16, no. 1, p. 233–238.

Castro, M. C., and Goblet, P., 2003, Calibration of regional groundwater flow models: Working toward a better understanding of site-specific systems: Water Resour. Res., v. 39, no. 6, art. 1172, doi: 10.1029/2002WR001653.

Castro, M. C., Goblet, P., Ledoux, E., Violette, S., and de Marsily, G., 1998b, Noble gases as natural tracers of water circulation in the Paris Basin 2. Calibration of a groundwater flow model using noble gas isotope data: Water Resour. Res., v. 34, no. 10, p. 2467–2483.

Castro, M. C., Jambon, A., de Marsily, G., and Schlosser, P., 1998a, Noble gases as natural tracers of water circulation in the Paris Basin 1. Measurements and discussion of their origin and mechanisms of vertical transport in the basin: Water Resour. Res., v. 34, no. 10, p. 2443–2466.

Chiles, J.-P., and Delfiner, P., 1999, Geostatistics. Modeling spatial uncertainty: Wiley, New York, 695 p.

Christensen, S., 1997, On the strategy of estimating regional-scale transmissivity fields: Ground Water, v. 35, no. 1, p. 131–139.

Davis, J. C., 2002, Statistics and data analysis in geology, 3rd ed.: Wiley, New York, 638 p.

Delhomme, J. P., 1974, La cartographie d'une grandeur physique à partir de données de différentes qualités (A cartographic method for assessing data with different reliabilities): Mémoires: Association Internationale des Hydrogéologues (Memoires: International Association of Hydrogeologists), v. 10, no. 1, p. 185–194.

Delhomme, J. P., 1979, Spatial variability and uncertainty in groundwater flow parameters; a geostatistical approach: Water Resour. Res., v. 15, no. 2, p. 269–280.

de Marsily, G., 1986, Quantitative hydrogeology: Academic Press, San Diego, 440 p.

Fabbri, P., 1997, Transmissivity in the geothermal Euganean Basin; a geostatistical analysis: Ground Water, v. 35, no. 5, p. 881–887.

Goovaerts, P., 1997, Geostatistics for natural resources evaluation: Oxford University Press, New York, 483 p.

Goovaerts, P., 1998, Ordinary cokriging revisited: Math. Geol., v. 30, no. 1, p. 21–42.

Goovaerts, P., 2000, Geostatistical approaches for incorporating elevation into the spatial interpolation of rainfall: J. Hydrol., v. 228, no. 1–2, p. 113–129.

Hamlin, H. S., 1988, Depositional and ground-water flow systems of the Carrizo–Upper Wilcox, South Texas, Report of Investigations 175: Bureau of Economic Geology, Austin, 61 p.

Hughson, L., Huntley, D., and Razack, M., 1996, Cokriging limited transmissivity data using widely sampled specific capacity from pump tests in an alluvial aquifer: Ground Water, v. 34, no. 1, p. 12–18.

Huntley, D., Nommensen, R., and Steffey, D., 1992, The use of specific capacity to assess transmissivity in fractured-rock aquifers: Ground Water, v. 30, no. 3, p. 396–402.

Isaaks, E. H., and Srivastava, R. M., 1989, An introduction to applied geostatistics: Oxford University Press, New York, 561 p.

Journel, A. G., 1980, The lognormal approach to predicting local distributions of selective mining unit grades: Math. Geol., v. 12, p. 285–303.

Journel, A. G., 1993, Geostatistics; roadblocks and challenges, *in* Soares, A., ed., Geostatistics Tróia '92, Quantitative Geology and Geostatistics: Kluwer Academic, Dordrecht, The Netherlands, v. 5, p. 213–224.

Journel, A. G., and Huijbregts, C. J., 1978, Mining geostatistics: Academic Press, London, 600 p.

Koltermann, C. E., and Gorelick, S. M., 1996, Heterogeneity in sedimentary deposits; a review of structure-imitating, process-imitating, and descriptive approaches: Water Resour. Res., v. 32, no. 9, p. 2617–2658.

Lavenue, M., and de Marsily, G., 2001, Three-dimensional interference test interpretation in a fractured aquifer using the pilot point inverse method: Water Resour. Res., v. 37, no. 11, p. 2659–2675.

Mace, R. E., 1997, Determination of transmissivity from specific capacity tests in a karst aquifer: Ground Water, v. 35, no. 5, p. 738–742.

Mace, R. E., and Smyth, R. C., 2003, Hydraulic properties of the Carrizo–Wilcox aquifer in Texas: Information for groundwater modeling, planning, and management, Report of Investigations 269: University of Texas at Austin, Bureau of Economic Geology, New Orleans, 40 p.

Neuman, S. P., 1982, Statistical characterization of aquifer heterogeneities; an overview, *in* Narasimhan, T. N., ed., Geol. Soc. Amer. Spectral Paper 189, p. 81–102.

Neuzil, C. E., 1994, How permeable are clays and shales?: Water Resour. Res., v. 30, no. 2, p. 145–150.

Patriarche, D., Castro, M. C., and Goblet, P., 2004, Large-scale hydraulic conductivities inferred from three-dimensional groundwater flow and ^{4}He transport modeling in the Carrizo aquifer, Texas: J. Geophys. Res., v. 109, no. B11, art. B11202, doi: 10.1029/2004JB003173.

Payne, J. N., 1972, Geohydrologic significance of Lithofacies of the Carrizo Sand of Arkansas, Louisiana, and Texas and the Meridian Sand of Mississippi, U. S. Geological Survey, Professional Paper 569-D: Washington, DC, 15 p.

Razack, M., and Huntley, D., 1991, Assessing transmissivity from specific capacity in a large and heterogeneous alluvial aquifer: Ground Water, v. 29, no. 6, p. 856–861.

Saito, H., and Goovaerts, P., 2000, Geostatistical interpolation of positively skewed and censored data in Dioxin-contaminated site: Environ. Sci. Technol., v. 34, no. 19, p. 4228–4235.

Wierenga, P. J., Hills, R. G., and Hudson, D. B., 1991, The Las-Cruces Trench site— Characterization, experimental results, and one-dimensional flow predictions: Water Resour. Res., v. 27, no. 10, p. 2695–2705.

Wladis, D., and Gustafson, G., 1999, Regional characterization of hydraulic properties of rock using air-lift data: Hydrogeol. J., v. 7, no. 2, p. 168–179.